

J. Veltman  
M. Stoutjesdijk  
R. Mann  
H. J. Huisman  
J. O. Barentsz  
J. G. Blickman  
C. Boetes

## Contrast-enhanced magnetic resonance imaging of the breast: the value of pharmacokinetic parameters derived from fast dynamic imaging during initial enhancement in classifying lesions

Received: 27 August 2007  
Revised: 31 December 2007  
Accepted: 15 January 2008  
Published online: 13 February 2008  
© The Author(s) 2008

J. Veltman (✉) · M. Stoutjesdijk ·  
R. Mann · H. J. Huisman ·  
J. O. Barentsz · J. G. Blickman ·  
C. Boetes  
Department of Radiology,  
University Medical Center Nijmegen,  
Geert Grooteplein-Zuid 10,  
6525 Nijmegen, GA, The Netherlands  
e-mail: j.veltman@rad.umcn.nl  
Tel.: +31-24-3614545  
Fax: +31-24-3540866

**Abstract** The value of pharmacokinetic parameters derived from fast dynamic imaging during initial enhancement in characterizing breast lesions on magnetic resonance imaging (MRI) was evaluated. Sixty-eight malignant and 34 benign lesions were included. In the scanning protocol, high temporal resolution imaging was combined with high spatial resolution imaging. The high temporal resolution images were recorded every 4.1 s during initial enhancement (fast dynamic analysis). The high spatial resolution images were recorded at a temporal resolution of 86 s (slow dynamic analysis). In the fast dynamic evaluation pharmacokinetic parameters ( $K^{\text{trans}}$ ,  $V_e$  and  $k_{ep}$ ) were evaluated. In the slow dynamic analysis, each lesion was scored according to

the BI-RADS classification. Two readers evaluated all data prospectively. ROC and multivariate analysis were performed. The slow dynamic analysis resulted in an AUC of 0.85 and 0.83, respectively. The fast dynamic analysis resulted in an AUC of 0.83 in both readers. The combination of both the slow and fast dynamic analyses resulted in a significant improvement of diagnostic performance with an AUC of 0.93 and 0.90 ( $P=0.02$ ). The increased diagnostic performance found when combining both methods demonstrates the additional value of our method in further improving the diagnostic performance of breast MRI.

**Keywords** Breast · MR · Dynamic · Pharmacokinetic

### Introduction

Breast cancer is the most commonly diagnosed cancer in women and the most prevalent cancer worldwide [1]. In breast imaging, mammography is still the most commonly used imaging techniques both in screening for and staging of breast cancer. However, dynamic contrast-enhanced magnetic resonance imaging (MRI) is becoming an increasingly important imaging modality in the detection and staging of breast cancer. Because of its superior sensitivity for the detection of invasive breast cancer, MRI has become a very important modality in breast imaging [2–5].

However, the classification of a lesion detected on MRI as benign or malignant still remains a challenge. Reported specificities in clinical studies range between 20% and 100% [6–15]. The main characteristics used for classifica-

tion of detected lesions on MRI are the lesion morphology and the enhancement dynamics [4]. Dynamic evaluation is often based on late dynamic characteristics of enhancing lesions. In this approach, the decrease of signal intensity, often referred to as a type 3 curve or washout, is highly suggestive for breast cancer with the likelihood for malignancy of 87% [12]. This dynamic evaluation makes use of high-resolution T1-weighted MRI images with a relatively low time resolution of 42 s or more [3, 12, 16–20]. The high spatial resolution of these sequences is necessary for accurate morphologic evaluation. Irregular lesion contour, inhomogeneous internal enhancement and rim enhancement have been described as features indicating a malignancy [21].

Schnall et al. [4] found focal mass margins and signal intensity to be a highly predictive imaging features.

However, the combination of both dynamic and morphological parameters resulted in the highest diagnostic accuracy in multivariate analysis.

The evaluation of early enhancement using a high temporal resolution has also been a subject of study in breast MRI. Boetes et al. [6] found in a group of 87 lesions a sensitivity of 95%, a specificity of 86% and an overall accuracy of 93% based on early enhancement characteristics. In this study, a temporal resolution of 2.3 s was achieved using a turboFLASH sequence. The value of a high temporal resolution during initial enhancement was confirmed by Sardanelli et al. [22] who used a temporal resolution of 15 s during the first minute of enhancement. The overlap between malignant and benign enhancement curves was only 9% using the fast dynamic evaluation compared with 50% using a lower temporal resolution of 1 min.

The value of first pass high temporal resolution imaging for the differentiation of benign and malignant lesions was studied in a direct comparison of steady-state dynamic MRI (30 s temporal resolution) and first-pass imaging (2 s temporal resolution) of induced mammary tumors in female rats by Helbich et al. [23]. In their study, an estimate of first-pass perfusion using T2\*-weighted imaging almost reached a significant difference between benign and malignant tumors. All other methods used, including T1-weighted first-pass imaging, failed to differentiate benign from malignant tumors. Gibbs et al. [24] also used a high temporal resolution (10.5–14.5 s) in the evaluation of small breast lesions and evaluated their data using a pharmacokinetic model. The incorporation of data from pharmacokinetic modeling in the evaluation of lesions improved diagnostic accuracy in their group.

High temporal resolution sequences often cover a limited area of the breast [6, 24]. These imaging protocols are, therefore, less suitable in clinical MRI or screening. For this study, we adjusted the scanning protocol in order to obtain a high temporal resolution during initial enhancement while covering both breasts entirely. The aim of this study is to assess the value of pharmacokinetic parameters derived from fast dynamic contrast enhanced imaging during initial enhancement in differentiating between benign and malignant breast lesions on MRI.

---

## Materials and methods

### Patient selection

All lesions detected on clinically performed breast MRI examinations in the period from January 2004 until June 2005 were initially included. All detected lesions were evaluated based on the following inclusion criteria: (1) histological confirmed diagnosis or (2) follow-up based on unchanged MRI morphology and enhancement characteristics during at least 24 months indicating a benign nature

of the lesion [25]. Lesions that could not be classified as benign or malignant using these criteria were excluded. The protocol was approved by the institutional review board.

### Imaging protocol

All patients were examined using a 1.5-Tesla MRI scanner (Sonata or Symphony, Siemens, Erlangen, Germany) in combination with a double breast coil. In premenopausal women, the MRI examination was performed in the second week of the menstrual cycle to minimize enhancement of normal glandular tissue [26]. Prior to the MRI examination, an intravenous catheter was inserted in the left or right arm. All patients were placed in the prone position with the breasts in the double breast coil and positioned at the isocenter of the magnet. After localizer images were obtained in three directions, low spatial resolution proton-density-weighted images were acquired in the transverse plane covering both breasts completely (TE 1.56, TR 800, FA 8, FOV 320, slices 24, TA 50 s, image resolution 3.9 mm×1.3 mm×4.0 mm). Subsequently, a coronally orientated high-resolution three-dimensional fast low-angle shot series (FLASH 3D) was acquired (TE 4, TR 7.5, FA 8, FOV 320, slices 120, TA 86 s, image resolution 1.3 mm×1.3 mm×1.3 mm). Thereafter, high temporal resolution T1-weighted images (turboFLASH) were recorded 22 times with identical spatial resolution and orientation as the proton-density-weighted images (TE 1.56, TR 66, FA 20, FOV 320, slices 24, TA 22×4.1 s) during an intravenous bolus injection of a paramagnetic gadolinium chelate—0.2 mmol of gadoterate meglumine (Dotarem; Guerbet, The Netherlands) per kilogram of body weight—which was administered with a power injector (Spectris; Medrad, Pittsburgh, USA) at 2.5 ml/s and followed by a 15-ml saline flush. Following these series, the FLASH 3D series was repeated four times. Total scan time for this protocol was 9 min 42 s, including the time needed to record localizer images.

### Image evaluation

For the evaluation, the MRI data were divided into two sets of dynamic data for each patient. The first dataset contained the high spatial resolution T1-weighted images (FLASH 3D) only. These were used for the evaluation of both lesion morphology as well as signal intensity versus time curves. This method will be further referred to as the ‘slow dynamic’ analysis. The second dataset contained the proton-density-weighted images, the high temporal resolution images as well as the precontrast high spatial resolution sequence. A high-resolution subtraction of the pre- and first postcontrast FLASH3D series prepared on the MRI scanner was also included in this dataset to aid in

lesion detection. The proton-density-weighted sequence was necessary for an accurate estimation of the T1 value necessary for the quantitative analyses. The evaluation of this dataset will be further referred to as the ‘fast dynamic’ analysis. In this fast dynamic analysis, the last three postcontrast FLASH 3D series were not used.

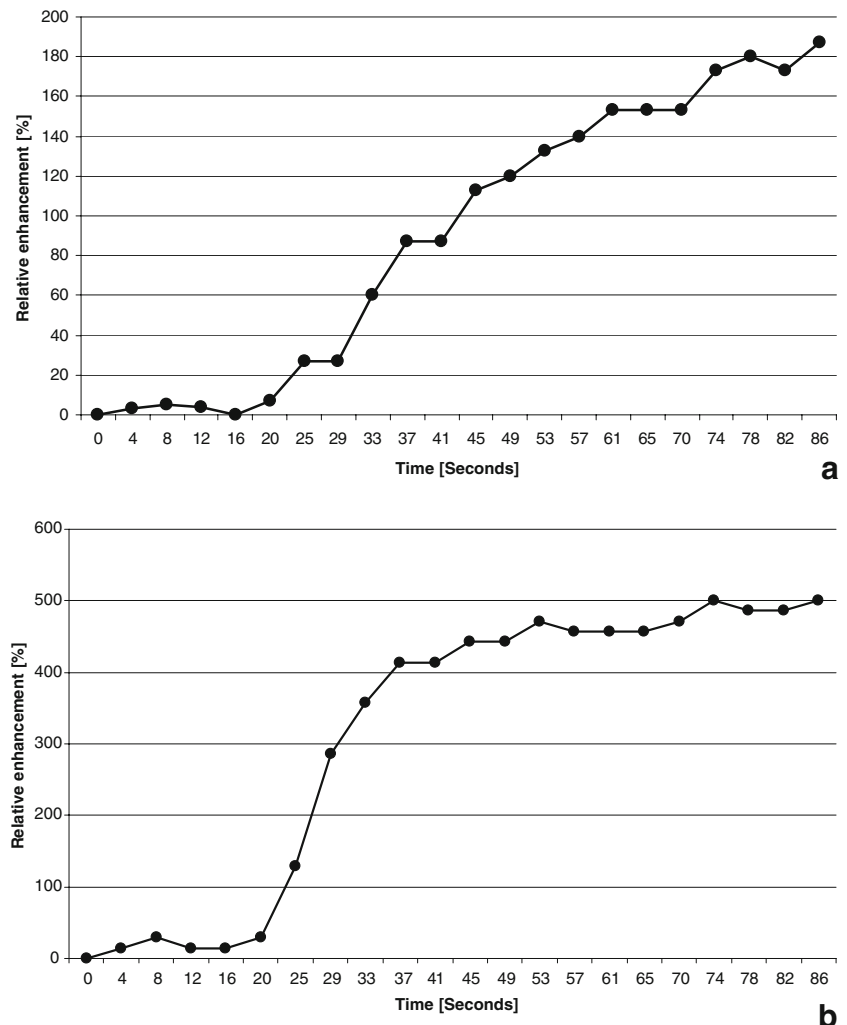
All cases were evaluated prospectively by two experienced breast MRI radiologists (reader 1 and reader 2). Both readers had over 5 years of experience in dynamic breast MRI. The evaluation on the two workstations was performed independently in different sessions with at least a 2-month time interval between both sessions.

For the slow dynamic analysis, a dedicated breast MRI workstation was used (Dynacad, Invivo, Germany). This workstation creates subtraction images for all time points after contrast administration, of which the first is automatically displayed together with the precontrast T1 acquisition, both in a coronal orientation. Furthermore, axial reconstructions were displayed for both the subtracted and T1-weighted images with color overlays of wash-in/

wash-out enhancement characteristics projected over the T1-weighted images [27]. A maximum intensity projection and signal intensity versus time curves were also displayed. This display protocol resembles the protocol used in the clinical workflow of dynamic breast MRI in our hospital. A BI-RADS classification was assigned for each lesion based on their morphology and enhancement dynamics [28]. No clinical information, mammography or prior MRI data were provided to the readers during the evaluation of the cases.

In the fast dynamic analysis, a workstation, developed in-house for the evaluation of dynamic contrast enhanced MRI, was used [29, 30]. On this workstation, pharmacokinetic parameters derived from the high temporal resolution turboFLASH series were automatically calibrated, calculated and displayed using color overlays. Examples of the recorded high temporal resolution enhancement versus time curves are presented in Fig. 1. In the preparation of this high temporal resolution data, each MRI signal enhancement/time curve was first fitted to a general

**Fig. 1** Relative enhancement versus time curves of a benign (a) and malignant (b) lesion. Note that the slope of enhancement and the level of enhancement is higher for the malignant lesion compared with the benign lesion. These fast dynamic acquisitions were analyzed as described in the [Materials and methods](#) section and resulted in the color overlays as presented in Figs. 4 and 5. The data used in this figure were respectively derived from a histopathology proven fibroadenoma and an invasive ductal carcinoma. The same lesions as presented in Figs. 4 and 5



exponential signal enhancement model, as described previously [31]. This reduces a curve to model with the following five parameters: baseline ( $s_0$ ); start of signal enhancement ( $t_0$ ), which defines the onset of the exponential curve; time-to-peak ( $ttp$ ), the exponential constant; peak enhancement ( $sp$ ), the signal amplitude at which the exponential curve levels off; and late wash, defined as the slope of the late part of the exponential curve. The reduced signal enhancement/time curve was converted to a reduced tracer concentration (mmol/ml)/time curve [31, 32], effectively converting  $sp$  to concentration tracer after initial rapid wash-in (often at a peak or plateau level) ( $C_{gd,p}$ ). The reduced plasma concentration time curve was estimated using the reference tissue method [33]. Deconvolution of the plasma profile and estimation of pharmacokinetic parameters conformed to the theoretical derivations [34], but was implemented in the reduced signal space as:  $V_e = C_{gd,p,tissue} / C_{gd,p,plasma}$ ;  $k_{ep} = 1 / (ttp_{tissue} - ttp_{plasma})$ .  $K^{trans} = V_e \times k_{ep}$ . Where  $V_e$  is an estimate of the extracellular volume [%],  $K^{trans}$ , the volume transfer constant (1/min), and  $k_{ep}$ , the rate constant (1/min), between extracellular extravascular and plasma space. The subscript 'tissue' stands for a measurement in the tissue under investigation and the subscript 'plasma' for the reference tissue plasma estimate. The reference tissue was automatically determined by selecting a set of voxels in the whole image volume [relative enhancement,  $(sp-s_0)/s_0$ ] larger than 0.2 and smaller than 2.0). This was most often the pectoral muscle, sometimes the liver or spleen. The additionally recorded proton density images were used to correct for the coil profile. The data were presented on the workstation with high-resolution precontrast T1-weighted images in an axial, coronal and sagittal reconstruction (FLASH 3D) as background. Color overlays were projected over the images representing  $K^{trans}$ ,  $k_{ep}$  and  $V_e$  parameter values that were based on the high temporal resolution images (turboFLASH). A subtraction image based on the pre- and first postcontrast FLASH 3D series was presented to aid in lesion detection. No criteria for differentiating between benign and malignant lesions were derived from the subtracted images. In this evaluation, the readers selected a region of interest (ROI) within the enhancing lesion. The ROIs were sphere-shaped and placed in an area within the lesion where the parameter values of  $K^{trans}$ ,  $V_e$  and  $k_{ep}$  were highest, based on the color-overlays. The outer limit of the lesion was used as a boundary of the ROI to rule out partial volume effects [35]. This method of ROI selection has previously been referred to as a hotspot method [36]. Each reader placed only one ROI per lesion. From this ROI, the workstation calculated the mean values for each of the pharmacokinetic parameters. Again, no clinical information, mammography or prior MRI data were provided to the readers during the evaluation of the cases. In case of multifocality, the tumor was analyzed as a single lesion.

## Statistical analysis

Differences in pharmacokinetic parameter values between the malignant and benign group were evaluated using an independent sample  $t$ -test. The performance of both methods was compared using a receiver operator characteristic (ROC) analysis. From the slow dynamic analysis, the reader's final BI-RADS classification of the lesion was used in the ROC evaluation; from the fast dynamic analysis, the mean parameter values calculated from the ROI selected by each reader were used. Multivariate analysis was performed using logistic regression in order to evaluate the possible additional value of both methods to one another. Since the differentiation between benign and malignant lesions is more difficult in smaller lesions a subgroup of all lesions of 2 cm and smaller were also separately evaluated. The comparison of the various results, including the interobserver variability, was done by using the area under the ROC curve (AUC) as an estimate of diagnostic accuracy. A pairwise comparison was performed to evaluate differences in the AUC.  $P$  values  $<0.05$  were considered to indicate statistical significance.

## Results

A total of 870 consecutive clinical breast MRI examinations in 787 patients were performed. In these studies a total of 188 lesions were detected. Eighty-six lesions could not be included due to lack of histological diagnosis or insufficient follow-up. This resulted in a total of 102 lesions in 96 patients; 34 benign and 68 malignant lesions. The mean age was 51 years (range 28–74 years). Ninety-four lesions were included based on histological evaluation, eight lesions based on follow-up. Mean lesion size on MRI for the malignant group was 32 mm (range 9–90 mm) and this was 15 mm (range 5–50 mm) for the benign

**Table 1** Histological composition of the benign and malignant group of lesions (*IDC* invasive ductal carcinoma, *DCIS* ductal carcinoma in situ, *ILC* invasive lobular carcinoma)

	Benign ( $n=34$ )	Malignant ( $n=68$ )	
Fibroadenoma	11	IDC	47
Fibrosis	4	DCIS	14
Adenosis	3	ILC	7
Inflammation	2		
Ductal papilloma	2		
Scar tissue	1		
Hyperplasia	1		
Hamartoma	1		
Radial scar	1		
Follow-up	8		

lesions. A total of 52 lesions were 2 cm or smaller; 25 malignant (mean lesion size 14 mm, range 6–20 mm) and 27 benign (mean lesion size 11 mm, range 5–20 mm).

The histological evaluation of the malignant lesions was in 14 cases based only on the core biopsy, in 14 cases based on an excision biopsy or breast saving surgery specimen and in 40 cases based on the mastectomy specimen. Histological proven benign lesions were in 19 cases based on a core biopsy and in seven cases based on an excision biopsy. Eight lesions were proven benign based on follow-up, mean follow-up was 37 months (range 24–52 months). The histological composition of the entire group is summarized in Table 1.

## Imaging results

In the slow dynamic analysis reader 1 classified 25 lesions as a BI-RADS 2 (benign:malignant=22:3), seven as BI-RADS 3 (4:3), 50 as BI-RADS 4 (6:44) and 20 as BI-RADS 5 (2:18). This was respectively 33 (24:9), 12 (4:8), 41 (5:36) and 16 (1:15) for reader 2. The ROC analysis for the slow dynamic analysis resulted in an AUC of 0.85 (95% CI=0.773–0.918) and 0.83 (95% CI=0.74–0.89) for reader 1 and 2, respectively.

The mean volume of the ROIs selected by the readers in the fast dynamic evaluation was 0.51 cm<sup>3</sup> for reader 1 (range 0.15–1.94 cm<sup>3</sup>, SD 0.30) and 0.52 cm<sup>3</sup> for reader 2 (range 0.15–1.94 cm<sup>3</sup>, SD 0.41). No significant difference was found for ROI size ( $P=0.72$ ). The pharmacokinetic parameters used in the fast dynamic analysis showed a significant difference between the benign and malignant group for both readers (Table 2). The diagnostic performance of the fast dynamic analysis resulted in an AUC for  $K^{\text{trans}}$  of 0.82 (95% CI=0.735–0.905) and 0.82 (95% CI=0.739–0.909) for reader 1 and 2. For  $V_e$  the AUC was 0.78 (95% CI=0.682–0.873) and 0.77 (95% CI=0.670–0.866)

**Table 2** Mean pharmacokinetic parameter values categorized for malignant and benign lesions per reader. All parameter values proved significantly higher in the malignant group compared to the benign group ( $P<0.01$ )

		Benign ( $n=34$ )	95% CI	Malignant ( $n=68$ )	95% CI
Reader 1	$K^{\text{trans}}$ <sup>a</sup>	1.2	0.9–1.4	2.3	2.1–2.6
	$V_e$	41.6	34.9–48.3	63.9	58.6–69.1
	$k_{\text{ep}}$ <sup>a</sup>	3.0	2.7–3.3	3.8	3.5–4.0
Reader 2	$K^{\text{trans}}$ <sup>a</sup>	1.3	1.0–1.5	2.5	2.2–2.8
	$V_e$	44.6	37.2–52.0	67.1	62.0–72.3
	$k_{\text{ep}}$ <sup>a</sup>	3.0	2.6–3.3	3.9	3.7–4.2

<sup>a</sup>1/min.

and for the  $k_{\text{ep}}$  parameter 0.72 (95% CI=0.609–0.828) and 0.74 (95% CI=0.629–0.841) for reader 1 and 2, respectively. Scatter plots of  $K^{\text{trans}}$  and  $V_e$  displaying the parameter values of benign and malignant lesions found in the two readers are provided in Fig. 2. The comparison of the diagnostic performance from the slow dynamic analysis with the single parameter fast dynamic analysis

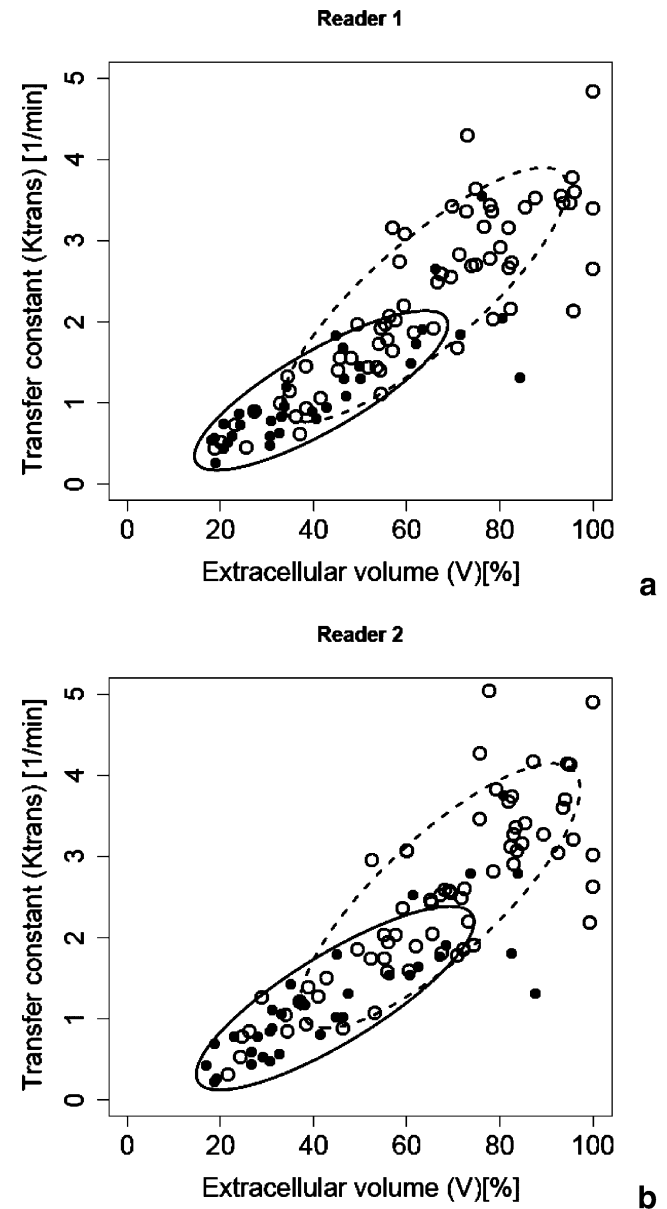


**Fig. 2** Scatter plots from the extracellular volume ( $V$ ) versus the transfer constant ( $K^{\text{trans}}$ ) for reader 1 (a) and reader 2 (b). Benign and malignant cases were clustered. Clusters were summarized with an iso-probability contour computed from the cluster mean and covariance at a squared normalized radius of 2. The *continuous-line ellipsoid* represents the benign subgroup, the *dotted-line ellipsoid* represents the malignant subgroup

showed no significant differences for the  $K^{\text{trans}}$  and  $V$  parameter. A significant difference was found for reader 1 between the slow dynamic analysis and the  $k_{\text{ep}}$  parameter ( $P=0.02$ ), the slow dynamic analysis showing better results. This was not found for reader 2 ( $P=0.08$ ).

Combining the pharmacokinetic parameters ( $K^{\text{trans}}$ ,  $K^{\text{ep}}$  and  $V$ ) in a multivariate analyses resulted in an AUC of 0.83 (95% CI=0.74–0.90) and 0.83 (95% CI=0.74–0.90) for reader 1 and 2. No significant difference was found between the multivariate fast dynamic and the slow dynamic diagnostic performance ( $P=0.49$  and  $P=0.85$ ).

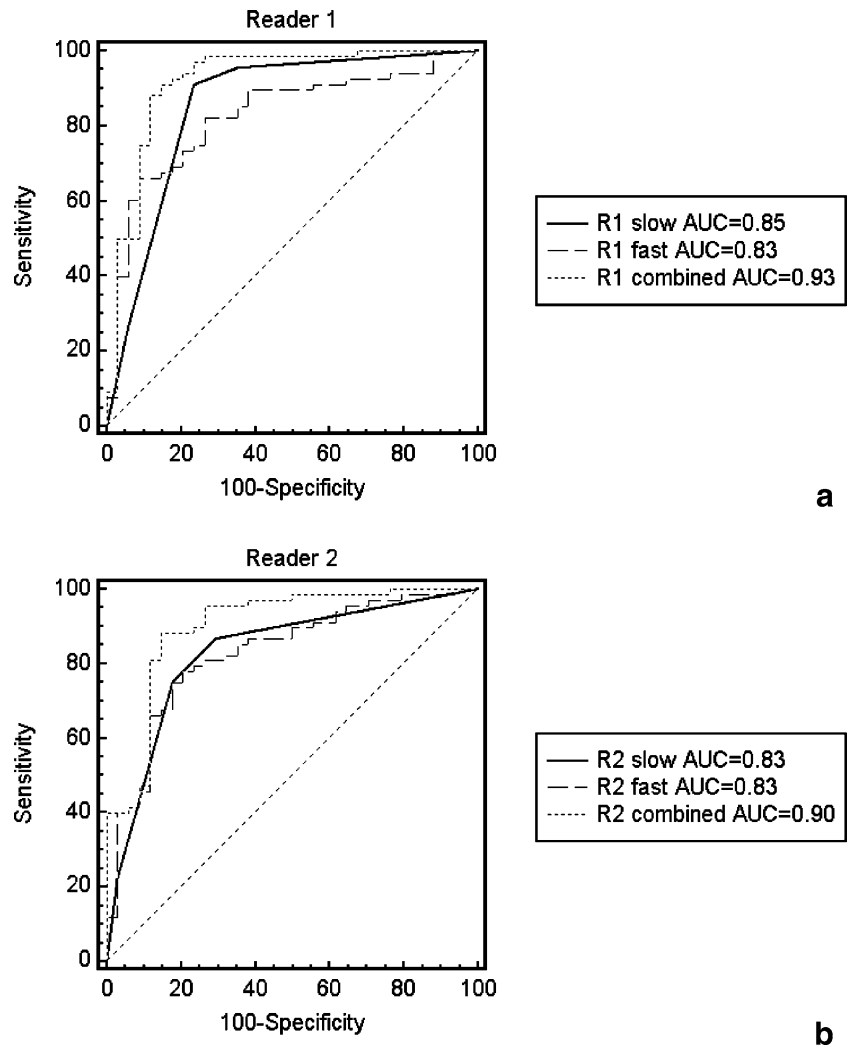
The multivariate analysis from all pharmacokinetic parameters combined with the slow dynamic analysis (combined analysis) resulted in an AUC of 0.93 (95% CI=0.85–0.96) and 0.90 (95% CI=0.83–0.95) for reader 1 and 2, respectively. The results from the combined analysis were significantly higher when compared with the fast dynamic analysis for both readers ( $P=0.01$  and  $P=0.02$ ). This was also found for the slow dynamic

analysis ( $P=0.02$  for both readers). The ROC curves are presented in Fig. 3.

In the group of lesions of 2 cm and smaller, the slow dynamic analyses resulted in an AUC of 0.87 (95% CI=0.75–0.95) for reader 1 and 0.79 (95% CI=0.67–0.91) for reader 2. Overall, the fast analyses resulted in this group in an AUC of 0.83 (95% CI=0.70–0.92) and 0.85 (95% CI=0.72–0.93), respectively. No significant difference was found between the slow and fast dynamic analyses for both readers ( $P=0.54$  and  $P=0.41$ ). The combined analysis resulted in an AUC of 0.97 (95% CI=0.88–0.99) and 0.94 (95% CI=0.84–0.99), respectively. The results from the combined analysis were significantly higher when compared with the fast dynamic analysis for both readers ( $P<0.01$  and  $P=0.04$ ). This was also found when compared to the slow dynamic analysis ( $P=0.03$  and  $P<0.01$ ).

No significant differences were found between the two readers in any of the analyses. An example of a benign and a malignant lesion is presented in Figs. 4 and 5.

**Fig. 3** ROC curve for reader 1 (a) and reader 2 (b) displaying the fast dynamic, slow dynamic and combined analysis. No significant differences were found between the fast and slow dynamic analysis in both readers. A significant difference was found between the slow dynamic analysis and the combined analysis for both readers ( $P=0.02$  for both readers). The comparison between the fast dynamic analysis and the combined analysis also resulted in a significant difference for both readers ( $P=0.01$  and  $P=0.02$ ). No significant differences were found between the two readers



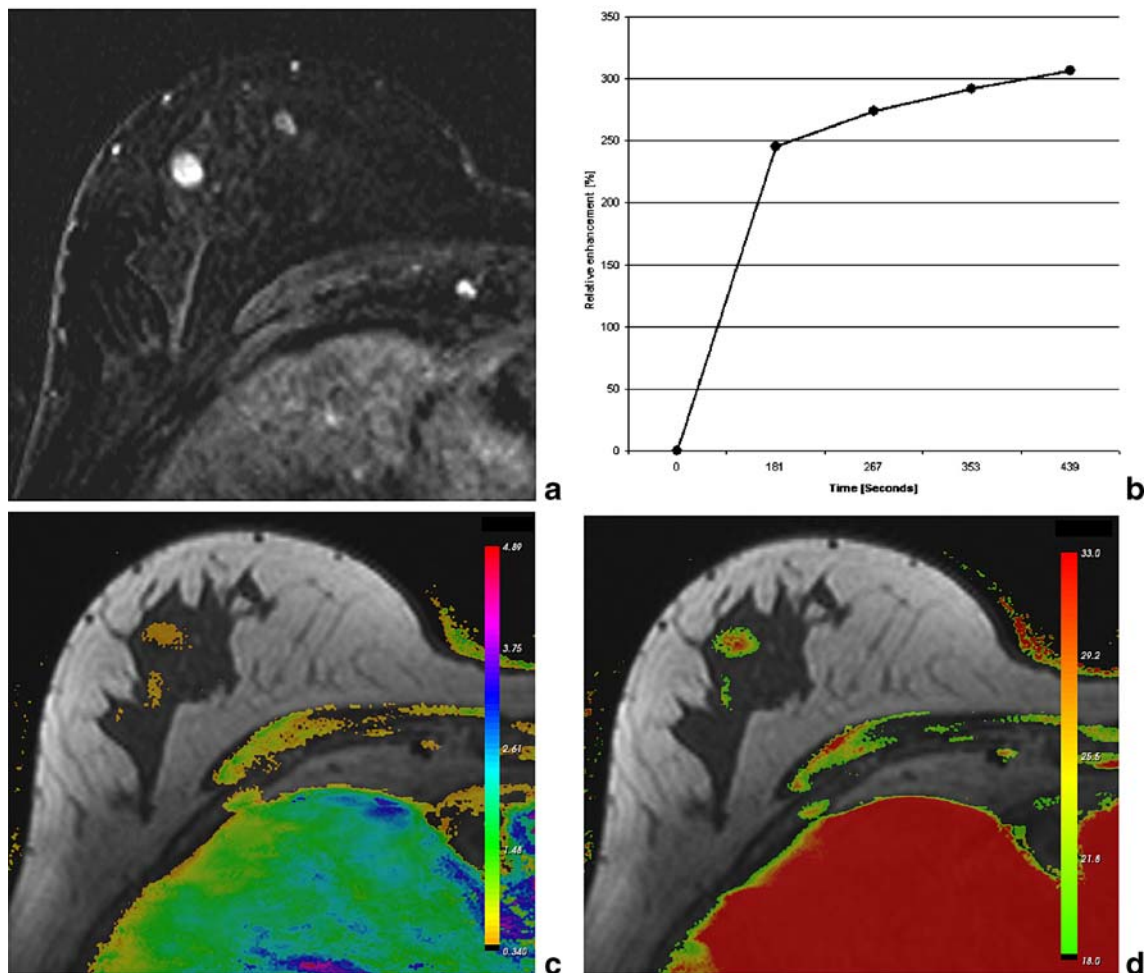


**Fig. 4** **a** Transverse reconstruction of the high-resolution subtraction sequence of the right breast. **b** Time versus relative enhancement curve of the slow dynamic series.  $K^{\text{trans}}$  (**c**) and  $V$  (**d**) color overlay images of the right breast, including a *scalar bar*, to demonstrate the parameter values. The subtraction image shows a rounded, mostly sharp delineated lesion. The time versus signal intensity curve demonstrates a type 1 curve, indicative for a benign

lesions. The readers classified this lesion as benign (BI-RADS 2) or probably benign needing follow up (BI-RADS 3) based on the slow dynamic analysis. The  $K^{\text{trans}}$  and  $V$  parameter color overlays demonstrate relatively low values for both parameters (see Table 2 for comparison) indicative for a benign lesion. Histopathology proved this lesion to be a fibroadenoma

## Discussion

In this study, we demonstrated that the pharmacokinetic parameters derived from fast dynamic scanning during initial enhancement were a valuable additional tool for the differentiation between benign and malignant breast lesions on MRI. The pharmacokinetic parameters were significantly higher for the malignant group compared with the benign lesions (Table 2). The diagnostic performance of the pharmacokinetic parameters was, compared with the results of the slow dynamic analysis, not significantly different. The combination of both methods, however, did improve the diagnostic performance significantly for both readers. These results were also found in the subgroup analysis of smaller breast lesions.

The slow dynamic analysis resembles the evaluation as routinely performed in the clinical workflow in our hospital. The performance of the workstation used in the slow dynamic evaluation has already been investigated and proven by Wiener et al. [27] in the evaluation of breast lesions prior to surgical treatment. Schnall et al. [4] evaluated the performance of both dynamic and morphological features in 854 women with 995 lesions. The results of their multivariate evaluation based on both morphological and relatively slow dynamic lesion characteristics resulted in a similar diagnostic accuracy (AUC values of 0.87 and 0.88) compared with the results obtained in the slow dynamic analyses of our study (0.85 and 0.83). Our results found in the slow dynamic analysis are, therefore, considered representative for the diagnostic performance of an experienced radiologist in this group of patients.

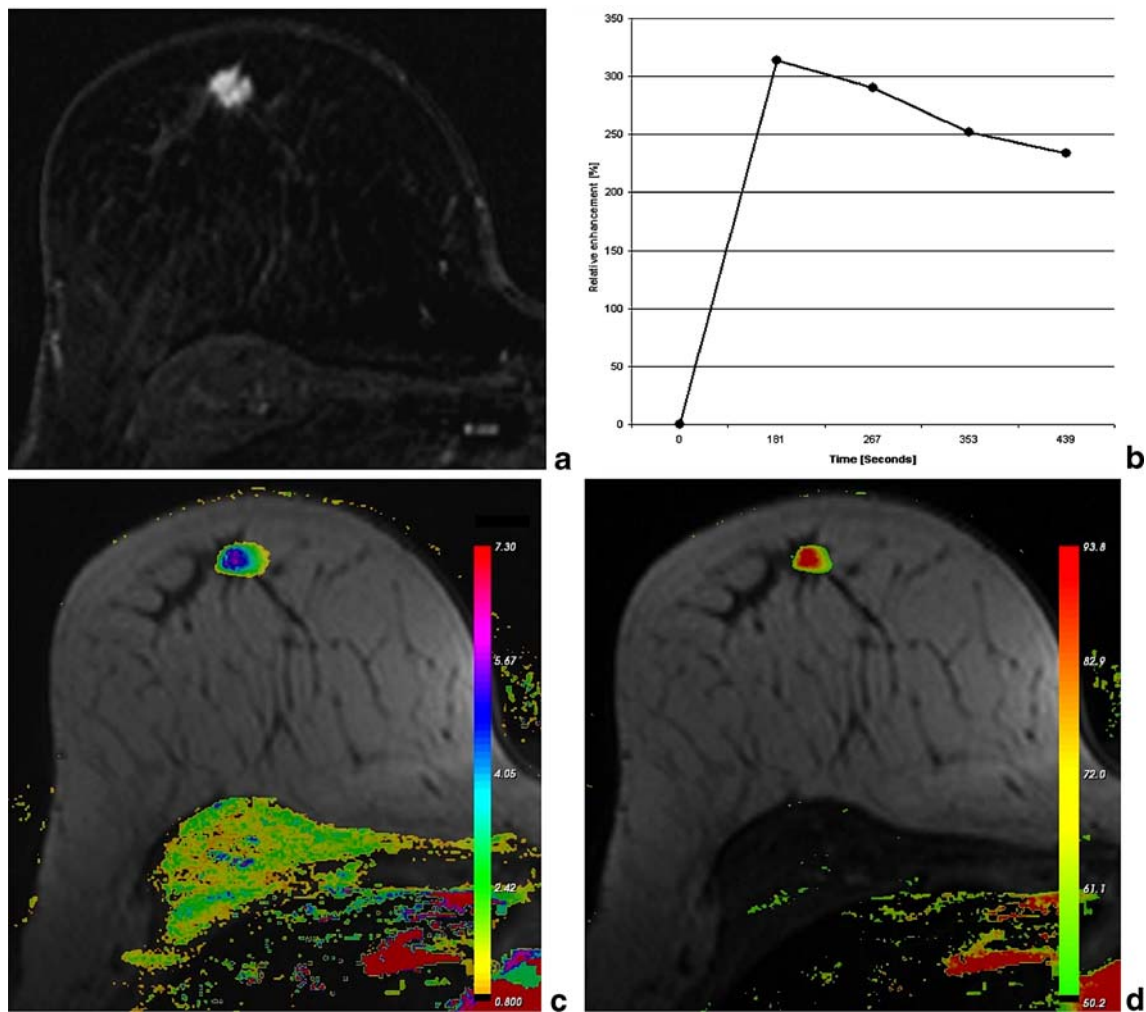


**Fig. 5** **a** Transverse reconstruction of the high-resolution subtraction sequence of the right breast. **b** Time versus relative enhancement curve of the slow dynamic series.  $K^{\text{trans}}$  (**c**) and  $V$  (**d**) color overlay images of the right breast, including a scalar bar, demonstrates the parameter values. The subtraction image shows a spiculated lesion retromammillar. The time versus signal intensity curve demonstrates a type 3 curve (wash-out) suggestive for a

malignancy. Both readers classified this lesion as malignant (BI-RADS 4) based on the slow dynamic analysis. The  $K^{\text{trans}}$  and  $V$  parameter color overlays demonstrate high values for both parameters (see Table 2 for comparison), indicative for a malignant lesion. Histopathology proved this lesion to be an invasive ductal carcinoma

In the fast dynamic analysis, both the morphologic characteristics and slow dynamic characteristics were not included in the evaluation; instead, a quantitative analysis of pharmacokinetic parameters was used based on manual ROI placement within the lesion. In the literature, both a “hot-spot” and “whole-tumor method for ROI placement are reported [36]. In this study, we used a hot-spot method. The importance of a consistent ROI placing strategy has been described by Liney et al. [36]. In our study, both readers were instructed with a simple ROI-placing strategy placing the ROI in an area with the highest parameter values guided by color overlays. Since no significant differences were found in the ROC analyses in any of the pharmacokinetic parameters used it is assumed that the performance of the fast dynamic analysis was not

negatively affected by this manual ROI selection strategy. The optimal strategy of ROI selection within a breast lesion is a subject that still needs to be further investigated; this is beyond the scope of this study.

Gibbs et al. [24] found the use of quantitative pharmacokinetic parameters in the evaluation of sub 1-cm breast lesions to be beneficial. In their study of 43 women, a diagnostic accuracy of 0.92 was found combining the postcontrast images with the dynamic data in a logistic regression analysis. The exchange rate constant was found to be the best individual parameter with a diagnostic accuracy of 0.74. The  $K^{\text{trans}}$  was also found to be the best individual parameter in our study with a diagnostic accuracy of 0.82. Furman-Haran et al. [18] concluded in their study of 141 lesions that the quantitative evaluation of



perfusion parameters should be able to improve breast cancer diagnosis on MRI. In their study the  $K^{\text{trans}}$  was also found to be the best discriminating parameter. Their analysis showed results of invasive ductal carcinoma versus fibroadenomas or fibrocystic changes. Unlike our study, the pharmacokinetic parameters used by Furman-Haran and coworkers were derived from high-resolution images with relatively a low temporal resolution of 2 min. Although our analysis used a more diverse histological distribution (Table 1) compared with the results presented by Furman-Haran et al. [18], only a relatively small number of benign lesions could be included. The diverse histological distribution also resulted in the inclusion of benign lesions that do not necessarily cause a diagnostic dilemma in daily practice. This can be seen as a limitation of our study. In the subgroup analysis of smaller lesions, a more equal distribution between benign and malignant lesions was found. The analysis performed in this subgroup also proved the additional value of the fast dynamic analysis in classifying small breast lesions on MRI.

The three-time-point method used by Kelcz et al. [37] provides the reader with a composite image showing contrast uptake and wash-out characteristics related to the product of microvessel surface area and permeability, as well as to the extracellular volume fraction. In their study, the observers correctly diagnosed 27 of 31 malignant and 31 of 37 benign lesions (sensitivity 87%; specificity 84%) using the three-time-point method. The evaluation based on wash-in and wash-out curves in combination with morphology resulted in a sensitivity of 93% and a specificity of 82%. Our results not only demonstrate a similar performance of the pharmacokinetic analysis compared with the evaluation based on morphology and slow dynamics but also demonstrate the potential gain if both methods are combined. The results presented by Kelcz et al. [37] are, like other authors, again derived from high spatial resolution images with a relatively low temporal resolution of 2 min compared with our fast dynamic scanning protocol.

With a scanning protocol using only the fast dynamic evaluation and morphology the scantime could be reduced significantly when compared with a protocol including the evaluation of wash-out. This without loss of diagnostic performance when compared with the results of the slow

dynamic analysis in our study and the results presented by other authors [4, 12, 18]. This reduction of scantime can in the future contribute to the cost-effectiveness of MRI screening. However, since the highest diagnostic performance was obtained by combining both the fast and slow dynamic analysis, further studies are needed before the scantime can be reduced.

The results presented in this study are our initial results using this scanning protocol. Therefore, no cut of values for the differentiation between benign and malignant lesions from the pharmacokinetic parameters were used in the evaluation or can be provided at this point. The results presented only show the potential of our method in differentiation between benign and malignant lesions in this group of patients. The value of our method needs to be further studied in a larger group, preferably using a more even distribution between benign and malignant cases and with lesions that can be classified on imaging as a BI-RADS 3 or higher.

Unfortunately, the study design used did not allow a multivariate analysis combining the fast dynamic data with morphological characteristics. Also, the possible trade-off between the pharmacokinetic parameters based on initial enhancement and the wash-out based on late dynamic characteristics cannot be derived from these data. Both analyses will need to be performed in future projects in order to evaluate the full potential of the fast dynamic analysis as used in our study. In conclusion, pharmacokinetic parameters derived from fast dynamic imaging during initial enhancement have great potential in classifying enhancing lesions in the breast. In this study, the diagnostic performance for the fast dynamic analysis proved to be equal to the results of experienced radiologists using more common evaluation methods based on morphologic characteristics and slow dynamic enhancement characteristics. An increased diagnostic performance was found in combining both methods. This shows the additional value of this method in further improving the diagnostic accuracy of breast MRI.

**Open Access** This article is distributed under the terms of the Creative Commons Attribution Noncommercial License which permits any noncommercial use, distribution, and reproduction in any medium, provided the original author(s) and source are credited.

## References

- Parkin DM, Bray F, Ferlay J, Pisani P (2005) Global cancer statistics, 2002. *CA Cancer J Clin* 55:74–108
- Boetes C, Veltman J, van Die L, Bult P, Wobbes T, Barentsz JO (2004) The role of MRI in invasive lobular carcinoma. *Breast Cancer Res Treat* 86:31–37
- Kriege M, Brekelmans CT, Boetes C, Besnard PE, Zonderland HM, Obdeijn IM, Manoliu RA, Kok T, Peterse H, Tilanus-Linthorst MM, Muller SH, Meijer S, Oosterwijk JC, Beex LV, Tollenaar RA, de Koning HJ, Rutgers EJ, Klijn JG (2004) Efficacy of MRI and mammography for breast-cancer screening in women with a familial or genetic predisposition. *N Engl J Med* 351:427–437
- Schnall MD, Blume J, Bluemke DA, DeAngelis GA, DeBruhl N, Harms S, Heywang-Kobrunner SH, Hylton N, Kuhl CK, Pisano ED, Causer P, Schnitt SJ, Thickman D, Stelling CB, Weatherall PT, Lehman C, Gatsonis CA (2006) Diagnostic architectural and dynamic features at breast MR imaging: multicenter study. *Radiology* 238:42–53
- Van Goethem M, Tjalma W, Schelfout K, Verslegers I, Biltjes I, Parizel P (2006) Magnetic resonance imaging in breast cancer. *Eur J Surg Oncol* 32:901–910
- Boetes C, Barentsz JO, Mus RD, Van Der Sluis RF, van Erning LJ, Hendriks JH, Holland R, Ruys SH (1994) MR characterization of suspicious breast lesions with a gadolinium-enhanced TurboFLASH subtraction technique. *Radiology* 193:777–781
- Gilles R, Guinebretiere JM, Lucidarne O, Cluzel P, Janaud G, Finet JF, Tardivon A, Masselot J, Vanel D (1994) Nonpalpable breast tumors: diagnosis with contrast-enhanced subtraction dynamic MR imaging. *Radiology* 191:625–631
- Heywang SH, Wolf A, Pruss E, Hilbertz T, Eiermann W, Permanetter W (1989) MR imaging of the breast with Gd-DTPA: use and limitations. *Radiology* 171:95–103
- Hulka CA, Smith BL, Sgroi DC, Tan L, Edmister WB, Semple JP, Campbell T, Kopans DB, Brady TJ, Weisskoff RM (1995) Benign and malignant breast lesions: differentiation with echo-planar MR imaging. *Radiology* 197:33–38
- Kaiser WA, Zeitler E (1989) MR imaging of the breast: fast imaging sequences with and without Gd-DTPA. Preliminary observations. *Radiology* 170:681–686
- Kelcz F, Santyr GE, Cron GO, Mongin SJ (1996) Application of a quantitative model to differentiate benign from malignant breast lesions detected by dynamic, gadolinium-enhanced MRI. *J Magn Reson Imaging* 6:743–752
- Kuhl CK, Mielcarek P, Klaschik S, Leutner C, Wardelmann E, Gieseke J, Schild HH (1999) Dynamic breast MR imaging: are signal intensity time course data useful for differential diagnosis of enhancing lesions? *Radiology* 211:101–110
- Nunes LW, Schnall MD, Orel SG, Hochman MG, Langlotz CP, Reynolds CA, Torosian MH (1997) Breast MR imaging: interpretation model. *Radiology* 202:833–841
- Perman WH, Heiberg EM, Grunz J, Herrmann VM, Janney CG (1994) A fast 3D-imaging technique for performing dynamic Gd-enhanced MRI of breast lesions. *Magn Reson Imaging* 12:545–551
- Fischer U, Kopka L, Brinck U, Korabiowska M, Schauer A, Grabbe E (1997) Prognostic value of contrast-enhanced MR mammography in patients with breast cancer. *Eur Radiol* 7:1002–1005
- Bedrosian I, Mick R, Orel SG, Schnall M, Reynolds C, Spitz FR, Callans LS, Buzby GP, Rosato EF, Fraker DL, Czerniecki BJ (2003) Changes in the surgical management of patients with breast carcinoma based on preoperative magnetic resonance imaging. *Cancer* 98:468–473
- Fischer U, Zachariae O, Baum F, von Heyden D, Funke M, Liersch T (2004) The influence of preoperative MRI of the breasts on recurrence rate in patients with breast cancer. *Eur Radiol* 14:1725–1731
- Furman-Haran E, Schechtman E, Kelcz F, Kirshenbaum K, Degani H (2005) Magnetic resonance imaging reveals functional divergence of the vasculature in benign and malignant breast lesions. *Cancer* 104:708–718
- Heywang SH, Hahn D, Schmidt H, Krischke I, Eiermann W, Bassermann R, Lissner J (1986) MR imaging of the breast using gadolinium-DTPA. *J Comput Assist Tomogr* 10:199–204
- Kuhl CK, Schild HH, Morakkabati N (2005) Dynamic bilateral contrast-enhanced MR imaging of the breast: trade-off between spatial and temporal resolution. *Radiology* 236:789–800
- Wedegärtner U, Bick U, Wörtler K, Rummeny E, Bongartz G (2001) Differentiation between benign and malignant findings on MR-mammography: usefulness of morphological criteria. *Eur Radiol* 11:1645–1650
- Sardanelli F, Rescinito G, Giordano GD, Calabrese M, Parodi RC (2000) MR dynamic enhancement of breast lesions: high temporal resolution during the first-minute versus eight-minute study. *J Comput Assist Tomogr* 24:724–731
- Helbich TH, Roberts TP, Gossmann A, Wendland MF, Shames DM, Adachi M, Yang S, Huber S, Daldrup H, Brasch RC (2000) Quantitative gadopentetate-enhanced MRI of breast tumors: testing of different analytic methods. *Magn Reson Med* 44:915–924
- Gibbs P, Liney GP, Lowry M, Kneeshaw PJ, Turnbull LW (2004) Differentiation of benign and malignant sub-1 cm breast lesions using dynamic contrast enhanced MRI. *Breast* 13:115–121
- Kopans DB (1994) Mammographic follow-up to detect breast cancer recurrence after conservative treatment. *Radiology* 190:286
- Kuhl CK, Bieling HB, Gieseke J, Kreft BP, Sommer T, Lutterbey G, Schild HH (1997) Healthy premenopausal breast parenchyma in dynamic contrast-enhanced MR imaging of the breast: normal contrast medium enhancement and cyclical-phase dependency. *Radiology* 203:137–144
- Wiener JJ, Schilling KJ, Adami C, Obuchowski NA (2005) Assessment of suspected breast cancer by MRI: a prospective clinical trial using a combined kinetic and morphologic analysis. *AJR Am J Roentgenol* 184:878–886
- American College of Radiology (2003) ACR BI-RADS: magnetic resonance imaging. In: *ACR Breast imaging reporting and data System*. American College of Radiology, Reston
- Fütterer JJ, Engelbrecht MR, Huisman HJ, Jager GJ, Hulsbergen-van de Kaa CA, Witjes JA, Barentsz JO (2005) Staging prostate cancer with dynamic contrast-enhanced endorectal MR imaging prior to radical prostatectomy: experienced versus less experienced readers. *Radiology* 237:541–549
- Fütterer JJ, Heijmink SW, Scheenen TW, Veltman J, Huisman HJ, Vos P, Hulsbergen-van de Kaa CA, Witjes JA, Krabbe PF, Heerschap A, Barentsz JO (2006) Prostate cancer localization with dynamic contrast-enhanced MR imaging and proton MR spectroscopic imaging. *Radiology* 241:449–458

31. Huisman HJ, Engelbrecht MR, Barentsz JO (2001) Accurate estimation of pharmacokinetic contrast-enhanced dynamic MRI parameters of the prostate. *J Magn Reson Imaging* 13:607–614
32. Hittmair K, Gomiscek G, Langenberger K, Recht M, Imhof H, Kramer J (1994) Method for the quantitative assessment of contrast agent uptake in dynamic contrast-enhanced MRI. *Magn Reson Med* 31:567–571
33. Kovar DA, Lewis M, Karczmar GS (1998) A new method for imaging perfusion and contrast extraction fraction: input functions derived from reference tissues. *J Magn Reson Imaging* 8:1126–1134
34. Tofts PS, Brix G, Buckley DL, Evelhoch JL, Henderson E, Knopp MV, Larsson HB, Lee TY, Mayr NA, Parker GJ, Port RE, Taylor J, Weisskoff RM (1999) Estimating kinetic parameters from dynamic contrast-enhanced T(1)-weighted MRI of a diffusable tracer: standardized quantities and symbols. *J Magn Reson Imaging* 10:223–232
35. Leach MO, Boggis CR, Dixon AK, Easton DF, Eeles RA, Evans DG, Gilbert FJ, Griebisch I, Hoff RJ, Kessar P, Lakhani SR, Moss SM, Nerurkar A, Padhani AR, Pointon LJ, Thompson D, Warren RM (2005) Screening with magnetic resonance imaging and mammography of a UK population at high familial risk of breast cancer: a prospective multicentre cohort study (MARIBS). *Lancet* 365:1769–1778
36. Liney GP, Gibbs P, Hayes C, Leach MO, Turnbull LW (1999) Dynamic contrast-enhanced MRI in the differentiation of breast tumors: user-defined versus semi-automated region-of-interest analysis. *J Magn Reson Imaging* 10:945–949
37. Kelcz F, Furman-Haran E, Grobgedl D, Degani H (2002) Clinical testing of high-spatial-resolution parametric contrast-enhanced MR imaging of the breast. *AJR Am J Roentgenol* 179:1485–1492